Spectroscopy of positive parity states in ^{26}Mg and ^{26}Al via the $(\alpha, ^3\text{He})$ and (α, t) reactions

M. Yasue
Research Center for Nuclear Physics, Osaka University, 10-1 Mihogaoka, Ibaraki, Osaka 567, Japan

K. Ogawa
Laboratory of Physics, Kantogakuin University, Kanazawa-ku, Yokohama 236, Japan

T. Niizeki, J. Takamatsu, M. Ohura, A. Terakawa, and T. Nakagawa
Department of Physics, Tohoku University, Sendai 980, Japan

T. Hasegawa
Faculty of Engineering, Miyazaki University, Miyasaki 889-21, Japan

H. Ohnuma and H. Toyokawa
Department of Physics, Tokyo Institute of Technology, Ohokayama, Tokyo 152, Japan

S. Hamada
Department of Nuclear Engineering, Kyoto University, Kyoto 606, Japan
(Received 1 May 1990)

The $(\alpha, ^3\text{He})$ and (α, t) reactions on ^{25}Mg were measured at $E_\alpha = 50$ MeV. Cross sections obtained for 57 positive parity states in ^{26}Mg and ^{26}Al were analyzed within the framework of the exact-finite-range distorted-wave Born approximation and compared to the full *s-d* shell model predictions. Reasonable agreement between the experimental strengths and the theory was obtained for the low lying states. Deviations of factors of 2 or more were found for some high lying 2^+, 3^+, and 4^+ states in ^{26}Al and especially for the 1_1^+ state in ^{26}Mg. The spectroscopic factors for the transitions to the analog states in ^{26}Mg and ^{26}Al were compared between these reactions. The same strength was obtained for the 6_1^-, $T=1$ state in ^{26}Mg and ^{26}Al, whereas an enhancement of about 30% was observed for the 0_1^+ and 3_1^+, $T=1$ states in ^{26}Al. Further, 1^+ states in ^{26}Mg proposed around $E_x = 10$ MeV through the (p,p') reaction were also observed in the $^{25}\text{Mg}(\alpha, ^3\text{He})$ reaction without the special enhancement for the 10.6 MeV 1^+ state seen in the (p,p') reaction. The total observed strengths for neutron stripping to the positive-parity states in the region of $E_x = 0$–11 MeV almost attained the limit of the pure *j-j* coupling scheme. Those for the proton stripping were 70% of the limit in the region of $E_x = 0$–8 MeV.

I. INTRODUCTION

Recently, Endt *et al.*[1,2] studied ^{26}Al in the region of excitation energy $E_x = 0$–8.1 MeV through the (p,γ) and (p,p') reactions on ^{25}Mg and made an extensive comparison of the experimental and calculated γ-ray strengths. The isoscalar $E2$ strengths[1] were well reproduced on average by the full *s-d* shell model calculation,[3] whereas the calculated isovector $M1$ strengths[1] were high by a factor of 1.85. Spectroscopic study of ^{26}Al through one-nucleon transfer reactions is another important and independent probe to investigate the validity of the shell model theory. One-nucleon stripping reactions on ^{25}Mg have been studied by several authors,[4,5] but detailed comparison with the shell model calculation remains unexplored.

In the present work, strengths for the transition to 31 positive-parity levels in ^{26}Al ($E_x = 0$–6 MeV) and for 26 levels in ^{26}Mg, which were deduced from the (α, t) and $(\alpha, ^3\text{He})$ reactions, respectively, are compared to the strengths estimated from Wildenthal's shell model.[3] Further, we will compare the strengths for the analog states of ^{26}Al and ^{26}Mg in order to see the higher-order configuration mixings in these states.

Previously, Kraushaar *et al.*[6,7] observed a meaningful difference between the spectroscopic factors for the $(\alpha, ^3\text{He})$ and (α, t) reactions leading to the 6_1^-, $T=1$ states in ^{26}Mg and ^{26}Al, respectively, and suggested an isospin mixed nature in these stretched particle-hole states. Their measurements[6,7] were carried out at different institutes. Here we will investigate the reactions under the same experimental condition and extend the comparison to the low-lying positive-parity analog states.

Another interest in this work is to see the $(\alpha, ^3\text{He})$ strengths for the 1^+ states in ^{26}Mg around $E_x = 10$ MeV, which were proposed by Crawley *et al.*[8] through the (p,p') reaction at $E_p = 201$ MeV. They observed 74% of the (p,p') strengths predicted for the 1^+ states in ^{26}Mg, and found that only the 10.64 MeV 1^+ states was selectively enhanced among the eighteen 1^+, $T=1$ states populated in the region of $E_x = 7$–15 MeV. The shell model calculation[3] also predicts a localization of the $0d_{3/2}$

single-particle strength for the neutron stripping to the 1^+ states around $E_x = 10$ MeV. However, any transfer reaction has not been investigated for the high-lying 1^+ states in ^{26}Mg according to the compilation.[9] We will deduce the spectroscopic factors for the 1^+ states in ^{26}Mg referring to the excitation energies proposed in the (p,p') experiment[8] and compare the strengths to the shell model calculations.[3]

II. EXPERIMENTAL PROCEDURE

The experiment was performed with a momentum-analyzed 50 MeV α-particle beam from the sector-focusing cyclotron at the Institute for Nuclear Study, of the University of Tokyo. Reaction products were analyzed by the quadrupole-dipole-dipole magnetic spectrometer[10] and detected with a drift-type single wire proportional counter[11] backed up by two ΔE counters and an E counter. An 80-μg/cm^2 (97.9% enriched) target of self-supporting ^{25}Mg foil was prepared by a rolling method. The thickness was calibrated by comparing the yields for elastic scattering with those from a ^{25}Mg foil whose thickness was measured to be 0.45 mg/cm^2 from the weight. The $(\alpha,{}^3\mathrm{He})$ and (α,t) reactions on ^{25}Mg were measured under the same experimental conditions. Typical momentum spectra at $\theta_{\mathrm{lab}} = 10°$ for the $(\alpha,{}^3\mathrm{He})$ reaction and at $\theta_{\mathrm{lab}} = 12.5°$ for the (α,t) reaction are shown in Fig. 1(a) and 1 (b), respectively, where the energy resolution is 25 keV at FWHM. Figure 1(c) shows a part of the $(\alpha,{}^3\mathrm{He})$ spectrum at $\theta_{\mathrm{lab}} = 7.5°$. The (α,t) spectrum in the region above $E_x = 6$ MeV was shown in our previous work.[12] Cross sections for 44 levels of ^{26}Mg and for 35 levels of ^{26}Al were deduced by a peak-fitting program.[13] An example of the fitting is presented in Fig. 1(d). The ambiguity in absolute values of the obtained cross sections is about 10%, but the relative errors are much smaller. Details of the experimental procedure are described elsewhere.[14]

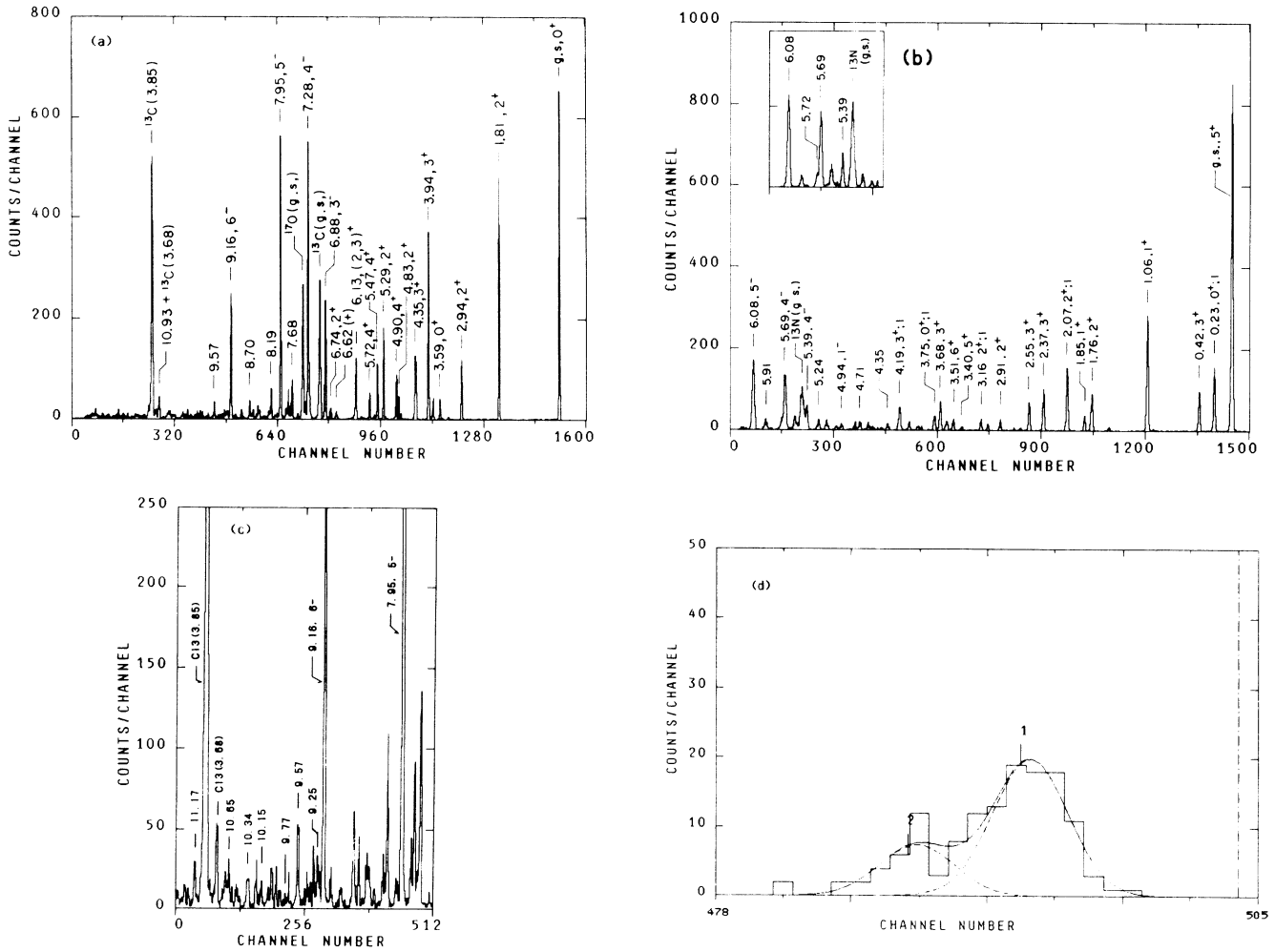

FIG. 1. (a) A momentum spectrum for the ^{25}Mg$(\alpha,{}^3\mathrm{He})^{26}$Mg reaction at $E_\alpha = 50.0$ MeV and $\theta_{\mathrm{lab}} = 10°$. (b) A momentum spectrum for the ^{25}Mg$(\alpha,t)^{26}$Al reaction at $E_\alpha = 50.0$ MeV and $\theta_{\mathrm{lab}} = 12.5°$. The inserted portion is a part of the spectrum at $\theta_{\mathrm{lab}} = 7.5°$. (c) A part of the spectrum for the $(\alpha,{}^3\mathrm{He})$ reaction at $\theta_{\mathrm{lab}} = 7.5°$. (d) A part of the $(\alpha,{}^3\mathrm{He})$ spectrum around $E_x = 5.7$ MeV at $\theta_{\mathrm{lab}} = 12.5°$. Closelying peaks for the 5.690 MeV 1^+ and the 5.716 MeV 4^+ states in ^{26}Mg are analyzed by keeping the peak shapes the same as that for the nearby single peak and by holding the separation of the peaks to be 26 keV. The labels 1 and 2 mean the peaks at $E_x = 5.690$ MeV and 5.716 MeV, respectively. Dashed and solid curves are calculated single peak shapes and the envelope of them, respectively.

III. ANALYSES

Angular distributions of the cross sections for the $(\alpha,{}^3\mathrm{He})$ and (α,t) reactions on ^{25}Mg were analyzed within the framework of the exact-finite-range DWBA using the code TWOFNR.[15] The parameters for the light particle systems of p-t and n-^{3}He in an α particle are described in Ref. 16. Potential parameters for the incident and the outgoing channels and for the form factors are listed in our previous work[12] on the ^{25}Mg$(\alpha,t)^{26}$Al reaction at $E_\alpha=50$ MeV. The parameters for the triton channel were assumed to be the same as for the ^{3}He channel.

Calculated cross sections are expressed as

$$\sigma_{\mathrm{calc}}=C^2s\sigma_{\mathrm{TWO}}\ , \tag{1}$$

where σ_{TWO} is the cross section calculated by the code TWOFNR. The isospin Clebsh-Gordan factors C^2 have values

$$C^2=1 \text{ for the } {}^{25}\mathrm{Mg}(\alpha,{}^3\mathrm{He})^{26}\mathrm{Mg} \text{ reaction},$$
$$=\tfrac{1}{2} \text{ for the } {}^{25}\mathrm{Mg}(\alpha,t)^{26}\mathrm{Al}\ (T=0 \text{ or } 1).$$

The light particle spectroscopic factor is $s=2$ for the $(\alpha,{}^3\mathrm{He})$ and (α,t) reactions. For the transitions to positive-parity states, a transfer of $0d_{5/2}$, $0d_{3/2}$, and $1s_{1/2}$ is allowed in the sd shell model space. In this case the value σ_{TWO} is a sum of the terms σ^j_{TWO} calculated for the transferred total angular momentum j.

$$\sigma_{\mathrm{TWO}}=\sum_j S^j_{\mathrm{calc}}\sigma^j_{\mathrm{TWO}}\ , \tag{2}$$

where the coefficient S^j_{calc} is the spectroscopic factor for the transfer of $0d_{5/2}$, $0d_{3/2}$, or $1s_{1/2}$ particles calculated from Wildenthal's shell model.[3] We carried out this shell model calculation with the code INS.[17] If the estimation is correct, the ratio of the experimental cross section σ_{expt} to the value σ_{calc} should be one. We will deduce the ratio

$$R=\sigma_{\mathrm{expt}}/\sigma_{\mathrm{calc}} \tag{3}$$

for each state in ^{26}Mg and ^{26}Al by normalizing the calculation to the data at forward angles.

For transitions to the negative-parity states we will deduce the spectroscopic factor S^j by fitting the σ_{calc} to the σ_{expt} values, as a reliable shell model calculation is not available to us in the larger model space of $sdfp$ shell orbits.

In case of transitions to unbound states, we used the zero-range (ZR) DWBA code DWUCK4,[18] which has an option of a resonance form factor for the unbound state. The cross section σ^j_{DW} calculated by this code is related to the value σ^j_{TWO} by

$$\sigma^j_{\mathrm{TWO}}=D_0^2\frac{2J_f+1}{(2j+1)(2J_i+1)}\sigma^j_{\mathrm{DW}}\ . \tag{4}$$

The D_0^2 value is set by comparing the calculated values σ_{TWO} and σ_{DW} for bound states as

$$D_0^2=14.0\times10^4\ \mathrm{MeV^2\,fm^3} \text{ for the } (\alpha,{}^3\mathrm{He}) \text{ reaction},$$
$$=13.2\times10^4\ \mathrm{MeV^2\,fm^3} \text{ for the } (\alpha,t) \text{ reaction},$$

where a finite range parameter of 0.7 fm and a nonlocal correction factor of 0.2 were used in the ZR DWBA calculation.[18]

IV. RESULTS AND DISCUSSION

Hitherto, several studies[4–7,12,19–22] of the one-nucleon stripping on ^{25}Mg were reported. Some[4,5,19–21] of them were carried out at low incident energies and restricted to the low-lying states. Others[6,7,12,22] at relatively high incident energies were concerned with the negative-parity high-spin states. Now Endt *et al.*[1,2] have presented a one-to-one correspondence of each level in ^{26}Al to the shell model calculation.[3] Such a correspondence helps us to carry out a detailed comparison of the experimental and theoretical spectroscopic factors for the states in ^{26}Al up to an excitation energy of about 6 MeV. In order to deduce reliable spectroscopic information from the experimental data, consistent DWBA analyses with a similar set of parameters and within the same framework are required. However, the previous work[4,5,19–21] did not follow such a consistency and have given varying strengths even for the transition to the 0^+_1, $T=1$ states in ^{26}Mg and ^{26}Al, ranging from 0.8 to 2.9.

Thus we will present the comparison with the shell model calculation by using our data and analyses. Following are the results for the states in ^{26}Mg and ^{26}Al observed in the present work. Our investigation spans the range of the excitation energies $E_x=0$–11 MeV in ^{26}Mg and $E_x=0$–9 MeV in ^{26}Al, where the data for the states in ^{26}Al above $E_x=6$ MeV are cited from our previous work[12] on the ^{25}Mg$(\alpha,t)^{26}$Al reaction.

A. 0^+, 2^+, 3^+, and 4^+ states of ^{26}Mg

Integrated cross sections and the ratio $\sigma_{\mathrm{expt}}/\sigma_{\mathrm{calc}}$ in Eq. (3) for the 0^+, 2^+, 3^+, and 4^+ states of ^{26}Mg are listed in Table I, where the E_x and J^π values are cited from Ref. 9. The spectroscopic factors calculated by the shell model[3] and the differences between the experimental and the theoretical excitation energies are also tabulated there. The $(\alpha,{}^3\mathrm{He})$ cross sections for these states are displayed in Figs. 2–5.

Angular distributions of the cross sections for the 0^+ states are well reproduced by the DWBA curves as seen in Fig. 2, and the strengths are consistent with the shell model predictions as listed in Table I. The 0^+_3 and 0^+_4 states are known at $E_x=4.972$ MeV and at $E_x=6.256$ MeV, respectively. Their cross sections are only 1% of those for the 0^+_1 state at forward angles. It is marvelous that the shell model calculation can reproduce such weak transitions to the 0^+_3 and 0^+_4 states. Angular distributions for these states were deduced at several angles only as their peaks in the spectrum were masked by the nearby larger ones at backward angles.

Transfers to the $0d_{5/2}$, $1s_{1/2}$, and $0d_{3/2}$ orbits are allowed in the transition to the 2^+ states. The DWBA calculations with the spectroscopic factors predicted by the shell model can reproduce the angular distribution shapes for the 2^+ states as seen in Fig. 3. The steep rise at forward angles for the 2.94 MeV 2^+_2 states is excellently ex-

TABLE I. Positive-parity states in ^{26}Mg observed via the $(\alpha,{}^3\mathrm{He})$ reaction at $E_\alpha = 50$ MeV.

E_x (MeV)	J^π[a]	σ_{INT} (mb)	S_{calc}[b] $0d_{5/2}$	$1s_{1/2}$	$0d_{3/2}$	$\sigma_{\mathrm{expt}}/\sigma_{\mathrm{calc}}$	ΔE_x[c] (MeV)
0	0_1^+	0.70	2.50			0.76	(0)
3.59	0_2^+	0.05	0.21			1.2	0.09
4.97	0_3^+	0.002	0.039			0.92	−0.23
6.26	0_4^+	0.003	0.055			0.98	0.20
1.81	2_1^+	0.66	0.42	0.04	0.01	1.07	−0.12
2.94	2_2^+	0.18	0.09	0.45	0.0007	1.0	−0.21
4.32	2_3^+	0.13[d]	0.058	0.018	0.0017	1.15[d]	−0.18
4.83	2_4^+	0.08	0.02	0.06	0.02	2.0	−0.17
5.29	2_5^+	0.27	0.03	0.03	0.42	1.07	−0.11
6.76	2_7^+	0.05	0.05	0.02	0.02	1.8	−0.08
7.10	2_8^+	0.007	0.0002	0.03	0.07	0.16	0.01
3.94	3_1^+	0.47	0.04	0.22	0.29	1.16	0.02
4.35	3_2^+	0.12	0.05	0.09	0.01	1.7	−0.16
6.12	3_3^+[e]	0.20	0.05	0.15	0.27	0.95	−0.14
or	(2_6^+)		(0.05	0.04	0.01)	(4.5)	(−0.52)
4.33	4_1^+	0.13[d]	0.03		0.05	1.15[d]	−0.20
4.90	4_2^+	0.18	0.009		0.175	0.8	−0.03
5.47	4_3^+	0.18	0.10		0.11	0.75	0.00
5.72	4_4^+	0.013	0.03		0	0.68	−0.29
6.62	(4_5^+)	0.05	0.008		0	5.5	−0.16
or	$(3^-,5^-)$						

[a]Cited from Ref. 9.
[b]Spectroscopic factors predicted in Wildenthal's shell model[3] were calculated using the shell model code INS.[17]
[c]$\Delta E_x = E_x^{\mathrm{expt}} - E_x^{\mathrm{calc}}$. The calculated value E_x^{calc} is normalized so that $\Delta E_x = 0$ for the ground state.
[d]Combined value for the 4.32 and 4.33 MeV doublet.
[e]Proposed in the present work.

plained to be due to the large $1s_{1/2}$ component. Cross sections for the 7.10 MeV 2_8^+ state are as small as $\frac{1}{100}$ of those for the 2_1^+ state, and have a large deviation from the calculation in strength and in angular distribution shape, suggesting some contributions of multistep processes for the transition to the 2_8^+ state. The peak for the 4.32 MeV 2_3^+ state was not separated from that for the 4.318 MeV 4_1^+ state in the present measurement and the combined results for these states are shown in Table I.

Figure 4 shows the cross sections for the 3^+ states. The compilation[9] informs us that the 6.12 MeV state has spin 2^+ or 3^+. If so, the state has a correspondence to the 2_6^+ or to the 3_3^+ state predicted by the shell model calculation, but the excitation energy of 6.12 MeV is more consistent with the calculated value for the 3_3^+ state rather than for the 2_2^+ state. The curve shown for the 6.12 MeV state represents the calculation for the 3_3^+ state. The calculation for the 2_6^+ state has not so steep a rise at forward angles as for the 3_3^+ state and cannot reproduce the data. The ratio of the experimental to the calculated cross section also prefers, as listed in Table I, the assignment of $J^\pi = 3^+$ to this state. Thus we propose the 6.12 MeV state to be the 3_3^+ state predicted by the shell model.

Cross sections for the 4^+ states are displayed in Fig. 5. They are well fitted by the calculated curves at forward angles but deviate from the curve at backward angles. The cross sections in the top view of the figure are for the doublet of the 4.318 MeV 4_1^+ and 4.332 MeV 2_3^+ states. The calculated curve for the doublet, which is derived by using the spectroscopic factors predicted by the shell model to the doublet, shows an excellent agreement with the experiment in strength as well as in angular distribution shape. The strengths for the other 4^+ states are well explained by the calculation except for the 6.62 MeV state. The compilation[9] points out the possibility of $J^\pi = 4^+$, 3^-, or 5^- to the 6.62 MeV state. The angular distribution shape for the 6.62 MeV state is, however, very similar to those for the other 4^+ states. Besides, the state is located very close to the position expected for the analog of the 6.818 MeV 4_5^+, $T=1$ state[1] in ^{26}Al. The difference is only 0.03 MeV. Thus the assignment of $J^\pi = 4^+$ is most probable for the 6.62 MeV state.

B. 1^+ states of ^{26}Mg

Recently Crawley *et al.*[8] proposed many 1^+ states in ^{26}Mg ranging from $E_x = 7.2$ to 15 MeV. On the other hand, the shell model calculation[3] predicts the 1_1^+, 1_2^+, and 1_3^+ states at $E_x = 5.83$ MeV, 6.79 MeV, and 7.72 MeV, respectively, in addition to the 1^+ states around $E_x = 10$ MeV. As shown in Table I, the deviation of the calculated E_x values from the experimental values is within 0.3 MeV at most. Hence, the 1_1^+ state should be

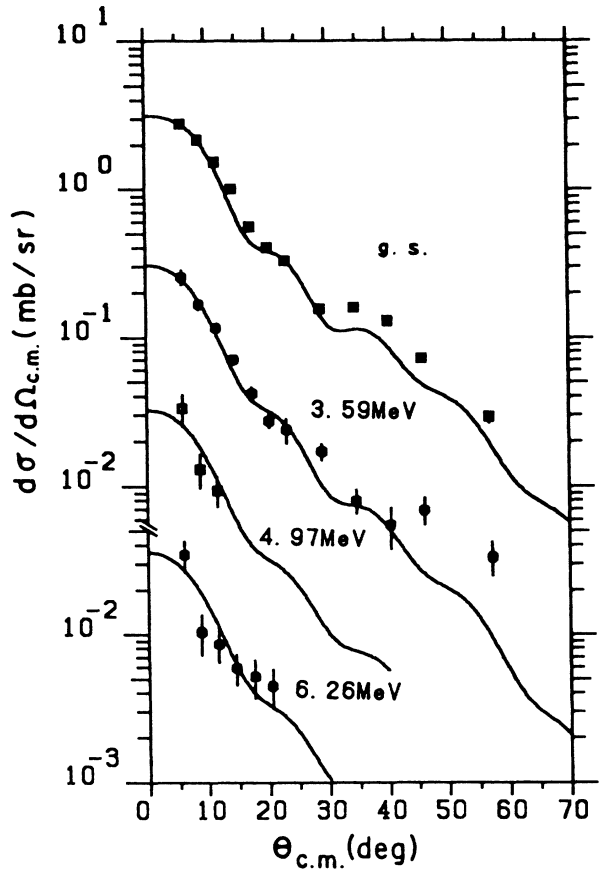

FIG. 2. Angular distributions of the cross sections for the ^{25}Mg(α,^{3}He)^{26}Mg reaction at $E_\alpha = 50$ MeV leading to the 0^+ states. Solid curves are exact-finite-range (EFR) DWBA calculations for a $0d_{5/2}$ transfer, which were carried out with the spectroscopic factors predicted from the shell model calculation. The curves are normalized to the data and the obtained normalizations are listed in Table I together with the predicted spectroscopic factors.

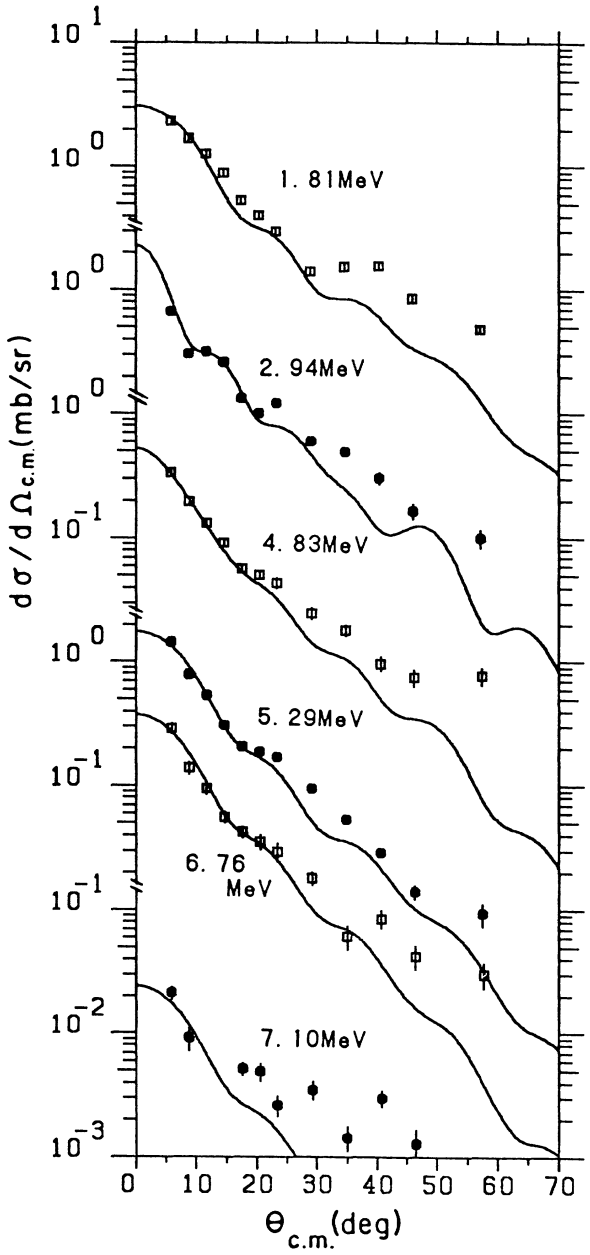

FIG. 3. Angular distributions of the (α,^{3}He) cross sections for the 2^+ states in ^{26}Mg. Curves are EFR-DWBA calculations carried out with the spectroscopic factors for the $0d_{5/2}$, $1s_{1/2}$, and $0d_{3/2}$ transfers in Table I. See the caption for Fig. 2.

expected around $E_x = 5.8$ MeV from the model.

Endt *et al.*[9] proposed the 5.690 MeV state to be of $1(2^+)$ from γ-decay strengths. The state is close to the 5.716 MeV 4_3^+ state and the cross section combined for the doublet was shown in Fig. 5. We have reanalyzed the data by assuming the doublet to be composed of the two peaks with a separation of 26 keV as demonstrated in Fig. 1(d). Obtained cross sections for each of these states are shown in Fig. 6, where the curve for the 5.72 MeV state is the DWBA calculation with the spectroscopic factors predicted for the 4_3^+ state. The results derived from the reanalyzed data for the 4_3^+ state are shown in Table I. The curve for the 5.69 MeV state represents the DWBA calculation for the $0d_{3/2}$ transfer and can reproduce the data without any $L=0$ component, supporting a proposal of the 5.690 MeV state to be the 1_1^+ state.

As discussed in the previous subsection, the 2_6^+ state predicted at $E_x = 6.64$ MeV by the shell model calculation is missing, and one may speculate the 5.69 MeV state to correspond to the predicted 2_6^+ state. The spectroscopic factors predicted for the 2_6^+ are listed at the line for the 6.12 MeV 3_3^+ state in Table I. The predicted value for the $1s_{1/2}$ transfer to the 2_6^+ state is comparable to that for the $0d_{5/2}$ transfer. If so, the angular distribution shape for the 2_6^+ state should show as steep a rise at forward angles as that for the 6.76 MeV 2_7^+ state displayed in Fig. 3. However, the 5.69 MeV data show rather pure $\Delta L = 2$ transfer and the excitation energy is

lower by 0.95 MeV than the value of 6.64 MeV predicted for the 2_6^+ state. The difference is too large to assign the 5.69 MeV state to the 2_6^+ state. Hence we propose this state to be the 1_1^+ state in comparison with the shell model calculation.

The angular distribution shape for the 7.697 MeV state is, as seen in Fig. 6, also described well by the $0d_{3/2}$ transfer, suggesting a possibility for the state to be the 1_3^+ state predicted by the shell model.

Figure 7 shows the cross sections for the states proposed to be 1^+ states by Crawley *et al.*,[8] where the curves are ZR-DWBA calculations for the $0d_{3/2}$ transfer. Although the excitation energies of these states are fairly consistent with those in Ref. 8, the $(\alpha,{}^3\mathrm{He})$ angular distribution shapes deviate largely from the curves except for the 9.256 MeV state. The obtained results for these

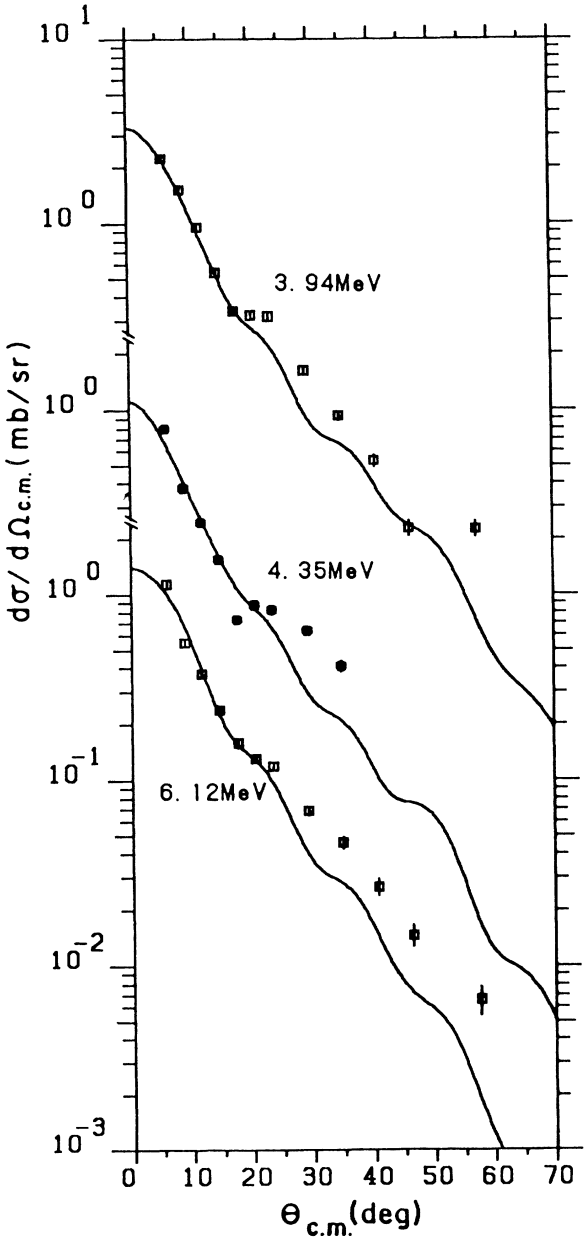

FIG. 4. Angular distributions of the $(\alpha,{}^3\mathrm{He})$ cross sections for the 3^+ states in ^{26}Mg. The 6.12 MeV state is proposed to be the 3_3^+ state in the present work. See the captions for Figs. 3 and 2.

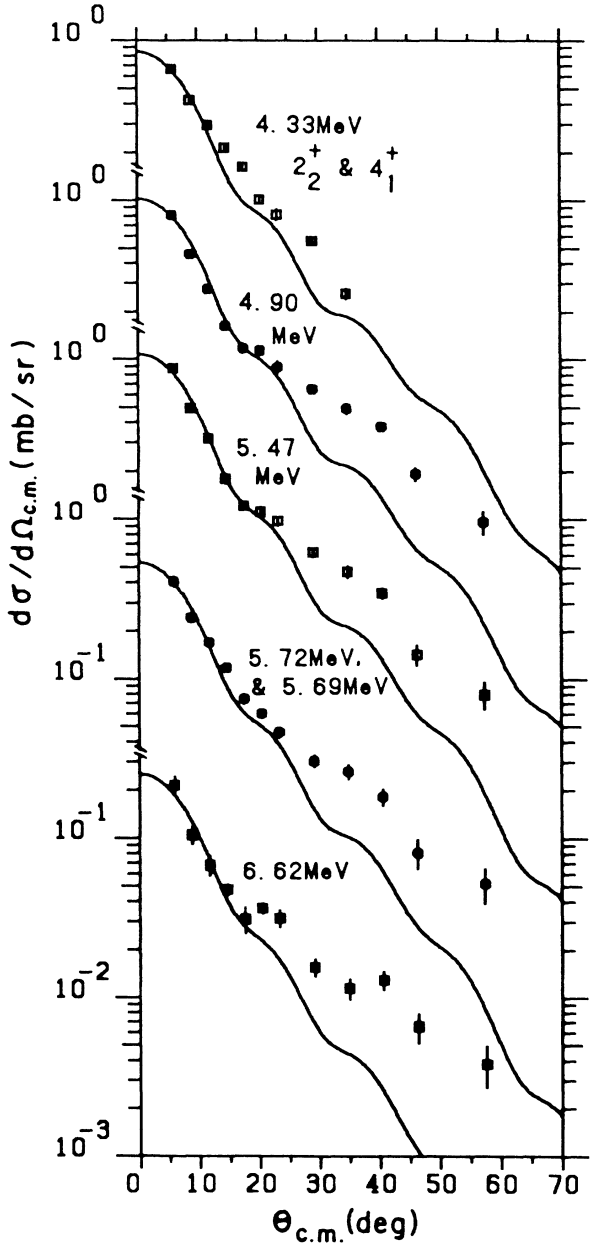

FIG. 5. Angular distributions of the $(\alpha,{}^3\mathrm{He})$ cross sections for the 4^+ states in ^{26}Mg. Curves are EFR-DWBA calculations with the spectroscopic factors in Table I. The 4.33 MeV data are the sum of yields for the 4.318 MeV 4_1^+ and the 4.332 MeV 2_3^+ states. The curve for the 4.33 MeV doublet is the sum of the calculated curves for the 4_1^+ and the 2_3^+ states. The 5.72 MeV data are the sum of the yields for the 5.716 MeV 4_4^+ and the 5.690 MeV 1_1^+ states. The yields for each member of the doublet are explicitly displayed in Fig. 6. See also the caption for Fig. 2.

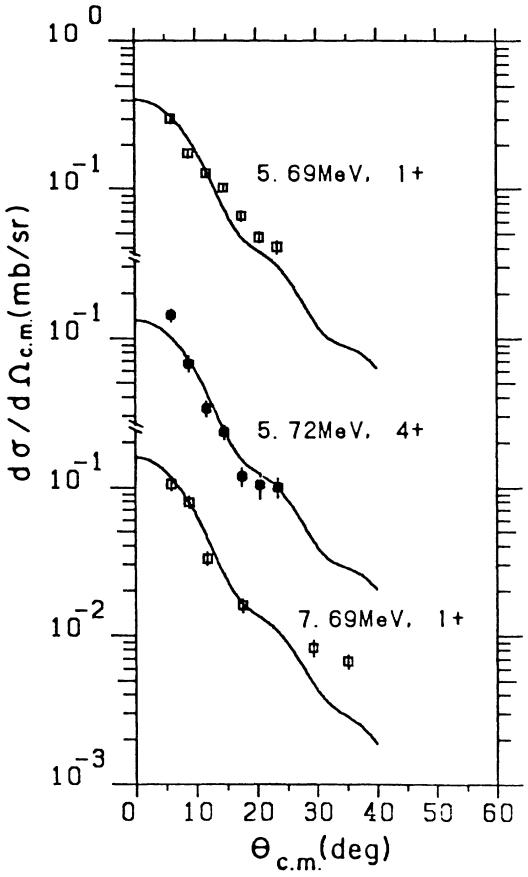

FIG. 6. Angular distributions of the $(\alpha,^3\mathrm{He})$ cross sections for the 5.69 MeV 1_1^+, 5.72 MeV 4_4^+ and 7.69 MeV 1_3^+ states in ^{26}Mg. The J^π value for the 5.69 MeV and the 7.69 MeV states is proposed in the present work. The curves for the 1^+ states are EFR-DWBA calculations for a $0d_{3/2}$ transfer and the deduced spectroscopic factors are listed in Table II. A DWBA calculation for the 4^+ state is carried out with the spectroscopic factors in Table I for the $0d_{5/2}$ and $0d_{3/2}$ transfers.

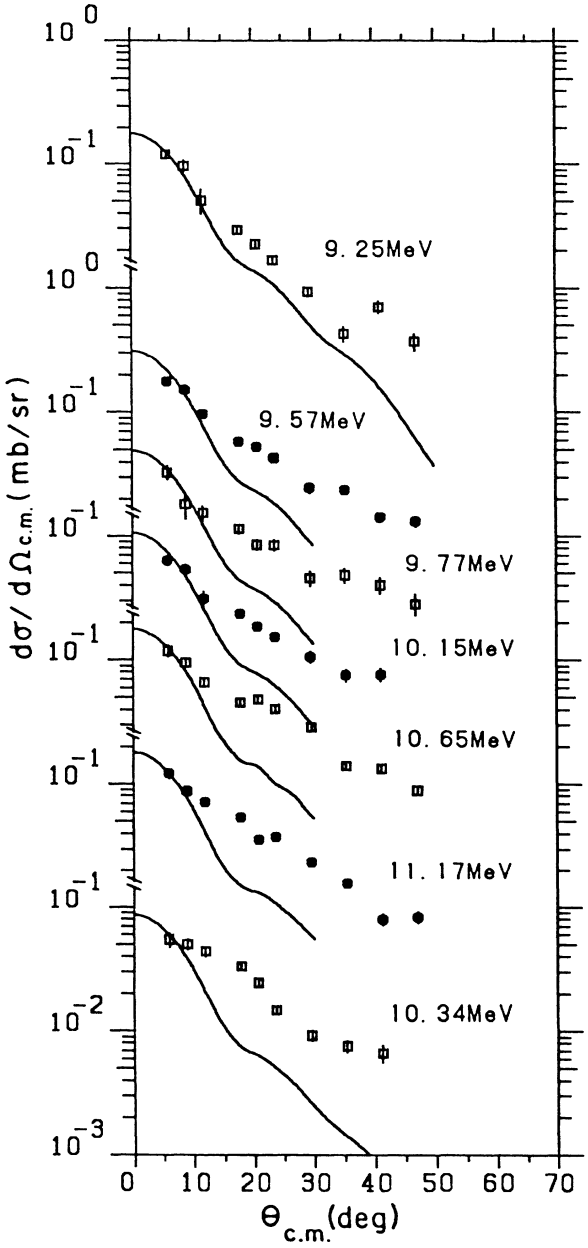

FIG. 7. $(\alpha,^3\mathrm{He})$ cross sections for the states which are proposed in the (p,p') scattering (Ref. 8) to be 1^+ states. Curves are ZR-DWBA calculations for a $0d_{3/2}$ transfer. Obtained spectroscopic factors are listed in Table II.

states are summarized in Table II and displayed in Fig. 8 with the spectroscopic factors predicted from the shell model.[3] The states with an asterisk in Table II are also excited by the (e,e') isovector $M1$ transition.[23] The (p,p') scattering can excite the 10.64 MeV 1^+, $T=1$ state in ^{26}Mg selectively among the fragmented 1^+ states due to the coherent interference of the amplitudes for the transition. On the other hand, the $(\alpha,^3\mathrm{He})$ reaction, which can sense only the $(d_{5/2}d_{3/2})$ component in the 1^+ states, is free from the interference and does not show such a selectivity as the (p,p') scattering. The shell model calculation also predicts the distribution of the $0d_{3/2}$ strength for the 1^+ states around $E_x=10$ MeV as displayed in Fig. 8. The predicted strengths for the $0d_{3/2}$ and $0d_{5/2}$ transfers to the 1^+ states are summed up to be 1.02, only 37% of the experimental value of 2.79. Especially the strength for the proposed 5.69 MeV 1_1^+ state is 46 times larger than the calculated strength.

Our results suggest that the shell model calculation cannot describe well the low-lying 1^+ states in ^{26}Mg, while the ratio of experimental to theoretical cross sections for (p,p') scattering to the 1^+ states in ^{26}Mg is 74%.[8] Namely, the (p,p') strengths for the 1^+ states around $E_x=10$ MeV are reasonably described by the calculation. The $(\alpha,^3\mathrm{He})$ cross sections for these high-lying 1^+ states have angular shapes much different from the shape expected from the direct transfer process. Larger $(\alpha,^3\mathrm{He})$ yields for the high-lying 1^+ states may come from multistep processes via the 2^+ states in ^{26}Mg. Such

an effect was shown for the $^{14}C(p,t)$ reaction[24] leading to the 1^+ state in ^{12}C.

C. Other positive-parity states in ^{26}Mg

Figure 9 shows the $(\alpha,^3He)$ cross sections for the states whose spin-parity is not known in the compilation.[9] Their angular distribution shapes are well fitted at forward angles by the DWBA curves for the transfer of $\Delta L=2$ and 0. Thus these states have positive parity.

In the figure, angular distributions for the 7.82, 8.25, and 9.05 MeV states are analyzed by assuming $0d_{3/2}$ and $1s_{1/2}$ transfer. Those for the other states are fitted by the DWBA curve for $0d_{3/2}$ transfer. In the former case, the calculated curves are fitted to the data at $\theta_{c.m.}=6°-35°$ by searching the spectroscopic factors for the $0d_{3/2}$ and $1s_{1/2}$ transfers. In this case, the fitted curves are too diffractive at backward angles and the deduced spectroscopic factors for the $1s_{1/2}$ transfer exceed the sum rule limit of the neutron number in the $1s_{1/2}$ shell orbit. Thus the angular distribution shapes at backward angles may not come from the component of the $1s_{1/2}$ transfer but from higher order reaction processes. Therefore we reanalyzed the data for the 7.82, 8.25, and 9.05 MeV data by fitting the calculated curve to the data at forward angles, $\theta_{c.m.}=6°-15°$ in order to deduce the components of direct transfer process. The spectroscopic factors deduced from the data at forward angles are listed in Table III.

TABLE II. Comparison of the $(\alpha,^3He)$ and (p,p') strengths for the 1^+, states in ^{26}Mg.

(p,p')[a]		$(\alpha,^3He)$[b]		
E_x (MeV)	$B(\sigma)$ (μ_n^2)	E_x (MeV)	σ_{INT} (mb)	Spectroscopic factor
		5.690	0.045	0.20
7.20	0.08			
7.42	0.14			
		7.697[c]	0.020	0.14
9.25[d]	0.31	9.256	0.031	0.29
9.58	0.54	9.568	0.070	0.57
9.79[d]	0.16	9.774	0.013	0.10
10.15[d]	0.73	10.147	0.024	0.26
10.32	0.20	10.340	0.026	0.23
10.64[d]	2.32	10.653	0.056	0.57
10.81	0.45			
11.15[d]	0.54	11.169	0.053	0.43
			⟨Sum⟩	⟨2.79⟩

[a]$M1$ reduced transition probabilities $B(\sigma)$ at $E_p=201$ MeV cited from Ref. 8.

[b]Present work. Spectroscopic factors were obtained for $0d_{3/2}$ transfer by using the zero-range DWBA code DWUCK4.[18] A resonance form factor is used for the unbound states above $E_x=11$ MeV. Errors in the excitation energy are 5 keV below $E_x=9$ keV and about 10 keV above $E_x=9$ MeV.

[c]$E_x=7.694$ MeV in a compilation.[9]

[d]Observed also by the (e,e') $M1$ transition.[24]

D. Negative-parity states of ^{26}Mg

Figure 10 displays the cross sections for the 6^-, 5^-, 4^-, 3^-, and 1^- states in ^{26}Mg whose J^π values are cited from the compilation[9] and from the previous work.[6,25,26] Shapes of the angular distributions for the 6^-, 5^-, and 4^- states are well reproduced with $0f_{7/2}$ transfer and those for the 3^- and 1^- states are with $0f_{7/2}$ and $1p_{3/2}$ transfers. Obtained results are compared in the upper half of Table IV with the previous work[6] on the $(\alpha,^3He)$ reaction at $E_\alpha=81$ MeV. Systematically, the present analysis gives larger spectroscopic factors than the previous one.

The cross sections for the states listed in the lower half of Table IV have angular distribution shapes characteristic of $\Delta L=3$ transfer, as shown in Fig. 11. These states are thus of negative parity.

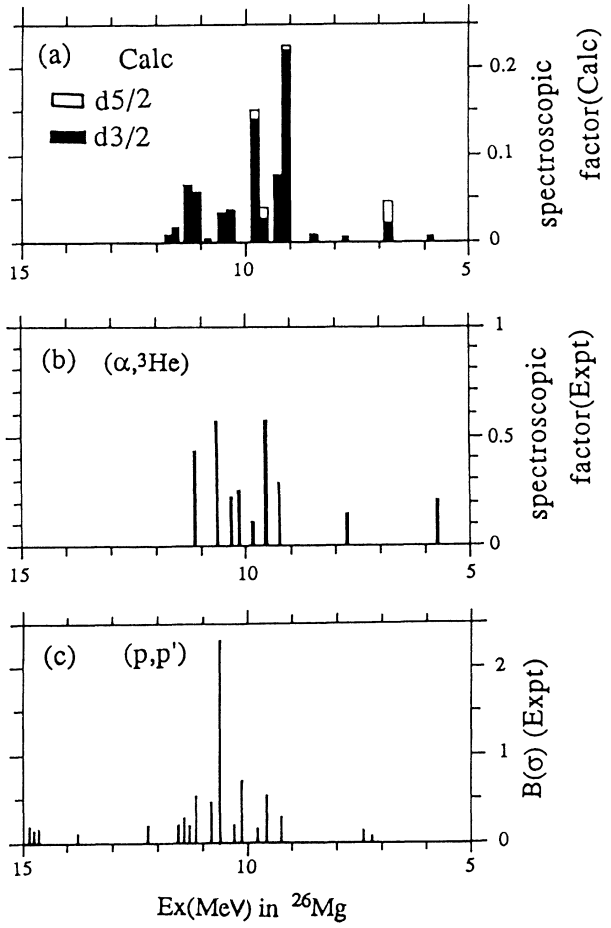

FIG. 8. Strengths of the transition to the 1^+ states in ^{26}Mg are compared between the $(\alpha,^3He)$ and (p,p') reactions. (a) Spectroscopic factors for the $0d_{3/2}$ and $0d_{5/2}$ transfer to the 1^+ states predicted by the shell model[3] with the code INS (Ref. 17). (b) Spectroscopic factors for the $0d_{3/2}$ transfer deduced from the $^{25}Mg(\alpha,^3He)^{26}Al$ reaction leading to the 1^+ states. (c) $M1$ reduced transition probability for the (p,p') scattering at $E_p=201$ MeV cited from Ref. 8.

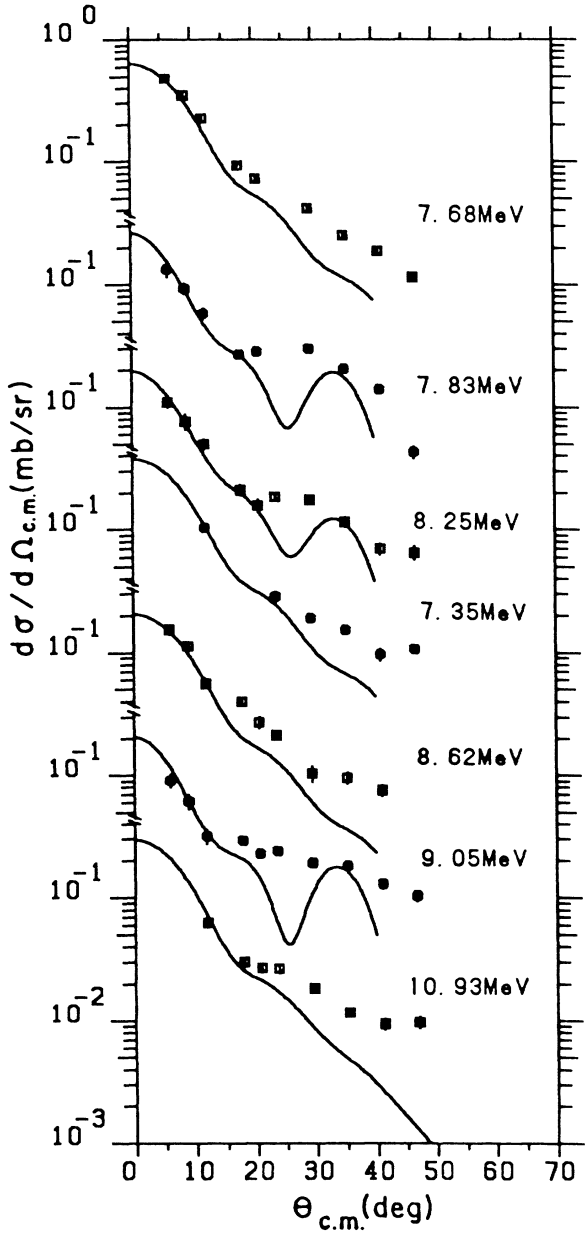

FIG. 9. Angular distributions of the $(\alpha,{}^3\mathrm{He})$ cross sections for the states whose spin values are not known, but their parity is proposed to be positive in the present work. See also explanations in the text.

E. Positive-parity states of ^{26}Al

Endt *et al.*[1,2] investigated the structure of ^{26}Al through the (p,γ) reaction and presented an extensive comparison with the *s-d* shell model calculation. In this section, we will make such a comparison in terms of the cross section strengths for the ^{25}Mg $(\alpha,t)^{26}$Al reaction.

Table V shows the states of ^{26}Al observed through the (α,t) reaction, where the spectroscopic factors calculated for the $0d_{5/2}$, $1s_{1/2}$, and $0d_{3/2}$ transfers from Wildenthal's shell model[3] are also tabulated. The cross sections estimated from these spectroscopic factors are compared to the data, and the ratio $\sigma_{\mathrm{expt}}/\sigma_{\mathrm{calc}}$ is tabulated there. In the table excitation energies of the observed states are compared to the values in Ref. 1. In most cases, the difference is within 5 keV.

The (α,t) transition to the 5^+ and 0^+ states in ^{26}Al is related to the $0d_{5/2}$ transfer within the assumption of the one-step reaction process. As seen in Fig. 12, the shape of the angular distribution for the 0.23 MeV 0^+, $T=1$ state has a good agreement with the calculation, while that for the 5^+ ground state has some deviation from the calculated curve at backward angles. Large deviation for the 3.40 MeV 5^+ state suggests an effect of higher order reaction processes. However, it is to be noted that the calculation can excellently reproduce the yields for these states at forward angles as seen in the ratio $\sigma_{\mathrm{expt}}/\sigma_{\mathrm{calc}}$ in Table V.

Cross sections for the four 1^+ states are displayed in Fig. 13. Angular distribution shapes for these states are well reproduced by the calculation. The ratio of the experimental to the calculated cross section is just one for the 1.06 MeV 1_1^+ state. Those for the other 1^+ states range from 1.2 to 1.4. A rather large value for the 5.01 MeV 1_6^+ state is due to the mixture of the yields for the 5.007 MeV 2^- state. The shell model can describe excellently strengths for the 1^+, $T=0$ states in ^{26}Al, while it cannot explain the yields for the low-lying 1^+, $T=1$ states in ^{26}Mg as discussed in Sec. IV B.

Cross sections for the eight 2^+ states are displayed with the calculated curves in Fig. 14. Their angular distribution shapes at forward angles are different from each other reflecting their strengths of the $1s_{1/2}$ component. The curves reproduce the angular distribution shapes

TABLE III. States in ^{26}Mg proposed to have a positive-parity via the $(\alpha,{}^3\mathrm{He})$ reaction at $E_\alpha=50$ MeV.

Previous work[a]	Present work			
E_x (MeV)	E_x (MeV)	σ_{INT} (mb)	$L2J$	Spectroscopic strength $(2J_F+1)S$
7.350	7.347	0.048	$D3$	1.0
7.674	7.676	0.118	$D3$	1.7
7.828	7.827	0.050	$D3$, $S1$	0.35, 5.4
8.249	8.247	0.034	$D3$, $S1$	0.35, 3.2
8.623	8.616	0.036	$D3$	0.64
9.046	9.048	0.040	$D3$, $S1$	0.20, 8.5
	10.931	0.034	$D3$	2.1

[a]Reference 9.

successfully. Besides, the calculation can describe the strengths of the 2^+ cross sections reasonably except for the 5.85 MeV 2_6^+ state. The cross section for the 3.751 MeV 2_4^+ state contains some yields for the 3.75 MeV 0_2^+, $T=1$ state. In fact, the centroid of the doublet was observed at $E_x=3.753$ MeV. Therefore we compared the cross section for the 3.75 MeV doublet to the value estimated from the spectroscopic factors for the 2_4^+ and 0_2^+ states. Thus we could obtain an excellent agreement between the data and the calculation in strength as well as in the angular distribution shape for the doublet.

In the present measurement, ten 3^+ states were observed below $E_x=6$ MeV. The only missed one is the 5.883 MeV, 3_{10}^+, $T=0$ state,[1] as the 5.883 MeV peak is masked by the tail of the larger 5.916 MeV 2^- peak. The yield for the 3_{10}^+ state is estimated to be at most $\frac{1}{4}$ of that for the nearby 5.849 MeV 2_6^+ state at $\theta_{lab}=5°$. The 3^+ angular shapes are well described by the calculation as seen in Fig. 15 except for the 0.42 MeV 3_1^+, the 4.35 MeV

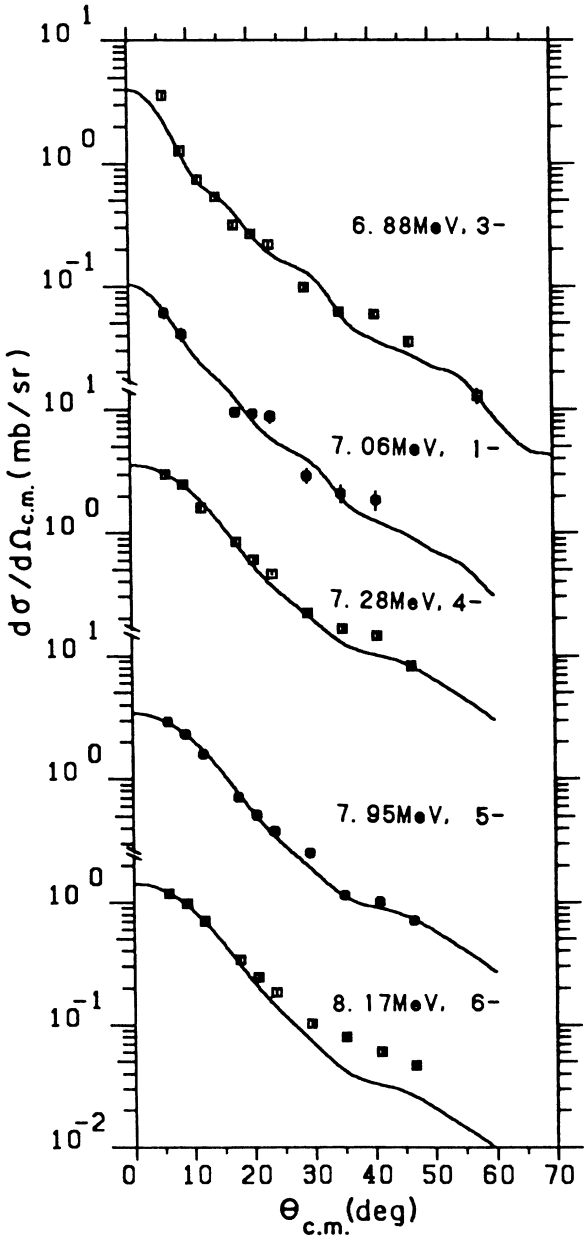

FIG. 10. Angular distributions of the $(\alpha,{}^3\mathrm{He})$ cross sections for the negative-parity states in ^{26}Mg. Curves for the 7.28 MeV, 7.95 MeV, and 8.17 MeV states are DWBA calculations for the $0f_{7/2}$ transfer. Those for the 6.88 MeV and the 7.06 MeV states are a sum of the DWBA calculations for the $0f_{7/2}$ and $1p_{3/2}$ transfers. Spectroscopic factors are listed in the top part of Table IV.

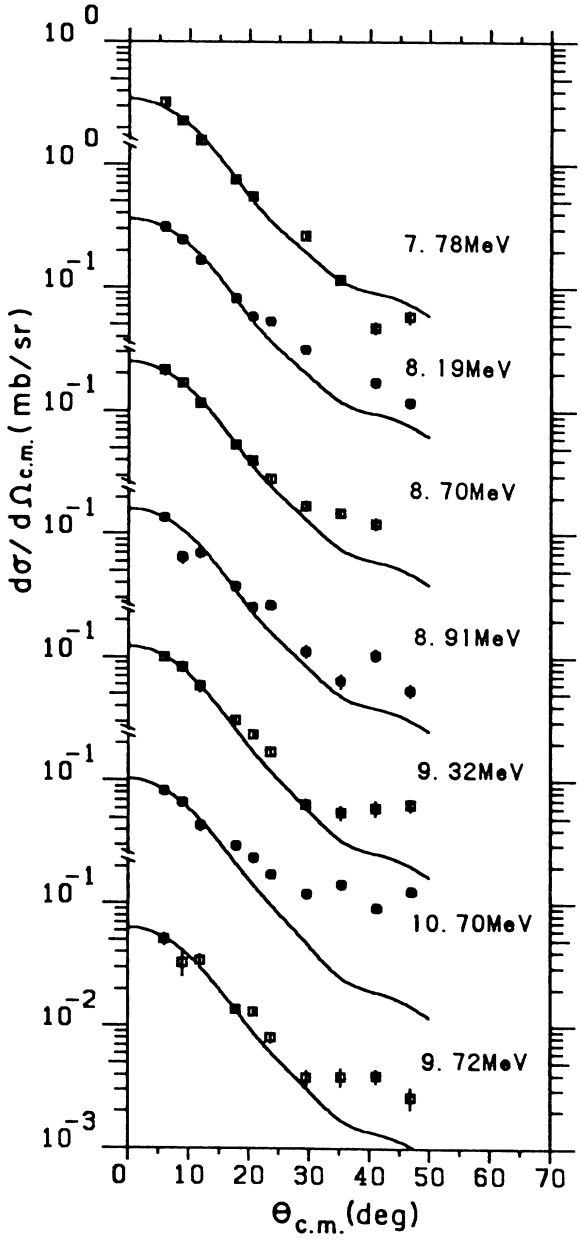

FIG. 11. $(\alpha,{}^3\mathrm{He})$ cross sections for the states whose spin-parity value is not known, but their angular distribution shapes are well reproduced by the DWBA calculations (solid curves) for the $0f_{7/2}$ transfer. Spectroscopic factors are listed in the lower part of Table IV.

TABLE IV. Upper part: Negative-parity states in ^{26}Mg observed via the $(\alpha,{}^3\mathrm{He})$ reaction at $E_\alpha=50$ MeV. Lower part: States of ^{26}Mg with transferred angular momentum $L=3$ in the $(\alpha,{}^3\mathrm{He})$ reaction at $E_\alpha=50$ MeV.

Previous work[a]		Present work			Spectroscopic factor (S) $(\alpha,{}^3\mathrm{He})$	
E_x (MeV)	J^π	E_x (MeV)	σ_{INT} (mb)	$L2J$	50 MeV	81 MeV[a]
6.878[b]	3^-	6.877	0.44	$F7$, $P3$	0.16, 0.99	
7.062[b]	1^-	7.062	0.014	$F7$, $P3$	0.01, 0.07	
7.279	4^-	7.279	0.84	$F7$	0.40	0.24
7.953	5^-	7.952	0.76	$F7$	0.36	0.21
9.169	6^-	9.165	0.36	$F7$	0.18	0.13

Previous work[b]	Present work		Spectroscopic strength[c]
E_x (MeV)	E_x (MeV)	σ_{INT} (mb)	$(2J_F+1)S$
7.771	7.775	0.077	3.9
8.183, 8.199	8.189	0.094	4.1
8.702	8.698	0.056	3.4
8.903, 8.929	8.914	0.038	2.2
	9.324	0.031	2.3
	9.716	0.016	1.2
	10.697	0.036	2.7

[a]Reference 6.
[b]Reference 9.
[c]$0f_{7/2}$ transfer is assumed.

3_8^+ and the 4.95 MeV 3_9^+ states. Larger $1s_{1/2}$ strength and the smaller $0d_{5/2}$ and $0d_{3/2}$ components than the prediction are required for the 3_1^+ state. In the ^{25}Mg $(^3\mathrm{He},d)$ ^{26}Al reaction at $E_h=18$ MeV, the angular distribution shape for the 3_1^+ state shows a pure $\Delta L=0$ pattern.[4] Cross section strengths for the lowest four 3^+, $T=0$ states and for the 3_1^+, $T=1$ state are well described by the calculation, while those for the other 3^+, $T=0$ states are two or three times larger than the calculations and that for the 3_7^+ state is only $\frac{1}{3}$ of the prediction. Too large $0d_{3/2}$ strength is predicted for the 3_7^+ state by the shell model calculation and too small $0d_{3/2}$ strengths are for the other high-lying 3^+ states. The ratio of the experimental to the calculated yields for the 3_{10}^+ states at $\theta_{\mathrm{lab}}=5°$ is also shown in Table V.

Figure 16 shows the cross sections for the 4^+ states, where the combined yields are given for the triplet of the 4_1^+, the 2_1^+, $T=1$ and the 1_3^+ states and for the doublet of the 4_2^+, $T=1$ and the 2_4^+, $T=1$ states. DWBA calculations for the composite states were carried out by taking account of the spectroscopic factors predicted to these states. Cross sections for the 4^+ states are well reproduced by the calculation in strength as well as in angular shape. One exception is seen in the strength for the 4_4^+ state.

Cross sections for the 3.51 MeV 6^+ and the 3.92 MeV $7^+(5^+)$ states are given in Fig. 17. Endt *et al.*[1] proposed that the assignment of $J^\pi=7^+$ to the 3.92 MeV state is preferred in comparison to the shell model prediction of their E_x values and also from the result on the (p,γ) experiment. The (α,t) angular distribution shape for the

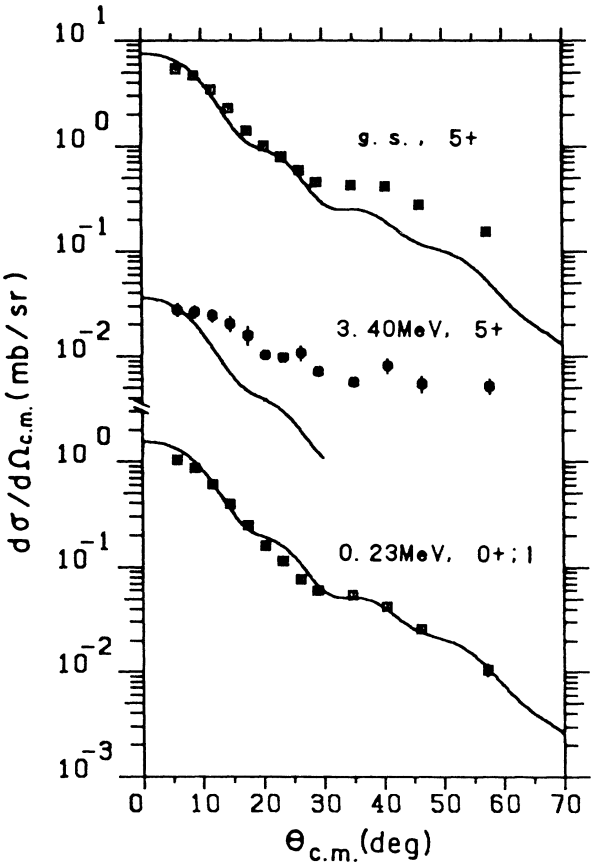

FIG. 12. Angular distributions of the cross sections for the ^{25}Mg$(\alpha,t)^{26}$Al reaction at $E_\alpha=50$ MeV leading to the 5^+ and 0^+ states. Solid curves are EFR-DWBA calculations for a $0d_{5/2}$ transfer, which were carried out with the spectroscopic factors predicted from the shell model calculation. The curves are normalized to the data and the obtained normalizations are listed in Table V together with predicted spectroscopic factors.

state is much different from those for the known 5^+ states in ^{26}Al. The (α,t) transitions to the 6^+ and 7^+ states in ^{26}Al are not allowed in the one-step one-nucleon transfer to the *sd* shell orbits. The yields for these states suggest some contributions of the higher ordered reaction process or a mixture of the higher shell orbits in the configuration of these states.

F. Negative-parity states of ^{26}Al

Cross sections for the 4.43 MeV, 2^- and the 4.48 MeV, 0^- states are also shown in Fig. 17 with the DWBA curves for the $0f_{7/2}$ and $0f_{5/2}$ transfers, respectively. The (α,t) reaction at $E_\alpha=50$ MeV could excite many negative-parity states above $E_x=5$ MeV. These states

TABLE V. States of ^{26}Al observed via the (α,t) reaction at $E_\alpha=50$ MeV in the region of $E_x=0$–6 MeV.

Previous work[a]		Present work[b]		S_{calc}			
E_x (MeV)	$J^\pi;T$	E_x (MeV)	σ_{INT} (mb)	$0d_{5/2}$	$1s_{1/2}$	$0d_{3/2}$	$\sigma_{expt}/\sigma_{calc}$
0	5_1^+	0	1.869	1.05			1.03
3.403	5_2^+	3.401	0.025	0.009			1.0
0.228	$0^+;1$	0.227	0.276	2.50			1.01
1.058	1_1^+	1.061	0.481	1.392		0.016	1.0
1.851	1_2^+	1.851	0.064	0		0.228	1.32
2.740	1_4^+	2.742	0.010	0		0.043	1.25
5.010	1_6^+	5.018	0.024	0.009		0.019	1.43
5.007	2^-						
1.759	2_1^+	1.758	0.216	0.048	0.317	0.299	1.43
2.661	2_2^+	2.659	0.014	0.006	0.019	0.050	0.56
2.913	2_3^+	2.913	0.049	0.001	0.076	0.095	1.25
3.160	$2_2^+;1$	3.162	0.053	0.088	0.449	0.001	1.0
3.751	2_4^+	3.753	0.084	0	0.157	0.234	1.0
3.754	$0_2^+;1$			0.206			
4.548	$2_3^+;1$	4.551	0.025	0.058	0.018	0.002	1.36
5.545	$2_5^+;1$	5.551	0.099	0.029	0.027	0.418	1.38
5.849	2_6^+	5.848	0.018	0.009	0.001	0	5.3
0.417	3_1^+	0.415	0.109	0.044	0.645	0.021	0.90
2.365	3_2^+	2.364	0.220	0.040	0.029	0.282	1.25
2.545	3_3^+	2.546	0.146	0.155	0.001	0.002	1.33
3.074	3_4^+	3.073	0.027	0.006	0	0.031	1.43
3.596	3_5^+	3.598	0.063	0.013	0.007	0.028	2.17
3.681	3_6^+	3.677	0.203	0.009	0.035	0.088	3.08
3.963	3_7^+	3.964	0.031	0.030	0.013	0.195	0.33
4.192	$3_1^+;1$	4.194	0.177	0.036	0.224	0.291	1.56
4.349	3_8^+	4.350	0.038	0.006	0	0.036	2.5
4.952	3_9^+	4.947	0.048	0.002	0.001	0.038	2.0
5.883	3_{10}^+	5.890		0.003	0.001	0.008	(0.9)
2.068	4_1^+			0.023		0.001	
2.069	$2_1^+;1$	2.066	0.28	0.348	0.039	0.014	1.07
2.072	1_3^+			0.012		0.068	
4.705	$4_1^+;1$	4.698	0.048	0.003		0.048	2.25
4.773	4_4^+	4.769	0.044	0.001		0.025	4.33
5.132	$4_2^+;1$		0.065	0.009		0.175	
5.142	$2_4^+;1$	5.145		0.022	0.061	0.020	0.89
5.245	4_5^+	5.261	0.063	0.056		0.051	1.9
5.726	$4_3^+;1$	5.730	0.043	0.102		0.111	0.46
3.508	6^+	3.511	0.105				
3.922	$7^+(5^+)$	3.926	0.074				
4.430	2^-	4.430	0.018				
4.480	0^-	4.482	0.005				

[a]Cited from Refs. 1,2, and 9.

[b]Other negative-parity states at $E_x=5.39$, 5.69, and 5.91 MeV are in our previous work (Ref. 12).

are reported in Ref. 12. We reanalyzed the previous data[12] with the same accuracy in the form factor calculation as in the present analyses. In Table VI the newly obtained spectroscopic factors for the 6^-, 5^-, and 4^- states in ^{26}Al, which are 20% smaller than those in Ref. 12, are compared to the other work on the (α,t) reaction[7] at $E_\alpha=81$ MeV and on the $(^3\text{He},d)$ reaction[22] at $E_h=55$ MeV. In spite of the difference of the range of momentum transfers in these reactions, the spectroscopic factors for the 6^- and 5^- states are excellently consistent with each other. Besides, the spectroscopic factor for the $0f_{7/2}$ transfer to the 9.26 MeV 6_1^-, $T=1$ state in ^{26}Al is nearly the same as the value for the 9.17 MeV 6_1^- state in ^{26}Mg as long as we refer to the values deduced in the present work for ^{26}Mg. Comparing the spectroscopic information in the upper half of Table IV and in Table VI, we can notice more fragmentation of the strengths for the $0f_{7/2}$ transfer to the states in ^{26}Al than in ^{26}Mg. The strength for the 5_1^- state in ^{26}Mg is larger than that for the 5_1^-, $T=0$ anti-analog state in ^{26}Al. It is fragmented to two levels in the case of the 5^-, $T=1$ states in ^{26}Al.

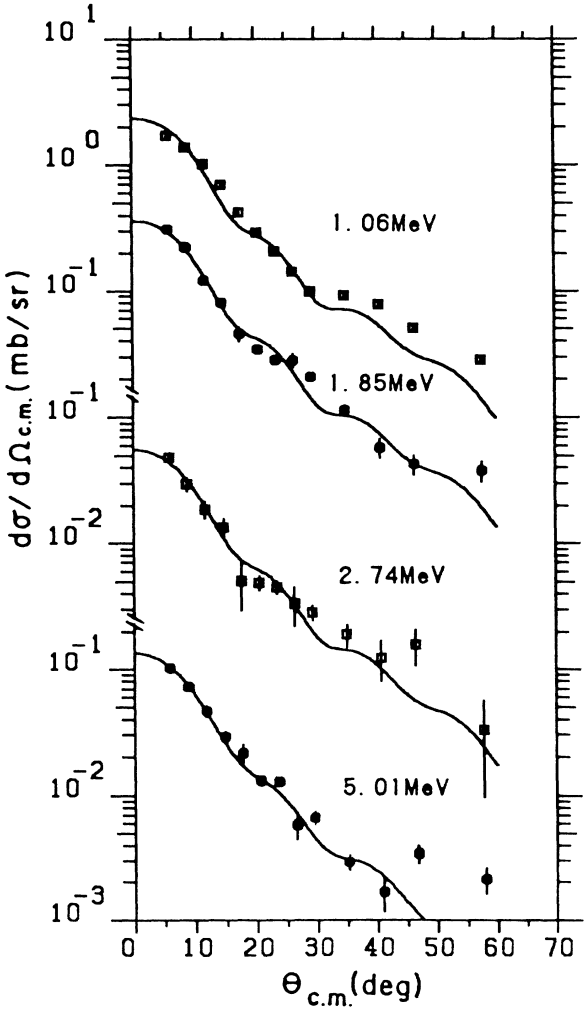

FIG. 13. Angular distributions of the (α,t) cross sections for the 1^+ states in ^{26}Al. Solid curves are EFR-DWBA calculations carried out with the spectroscopic factors in Table V.

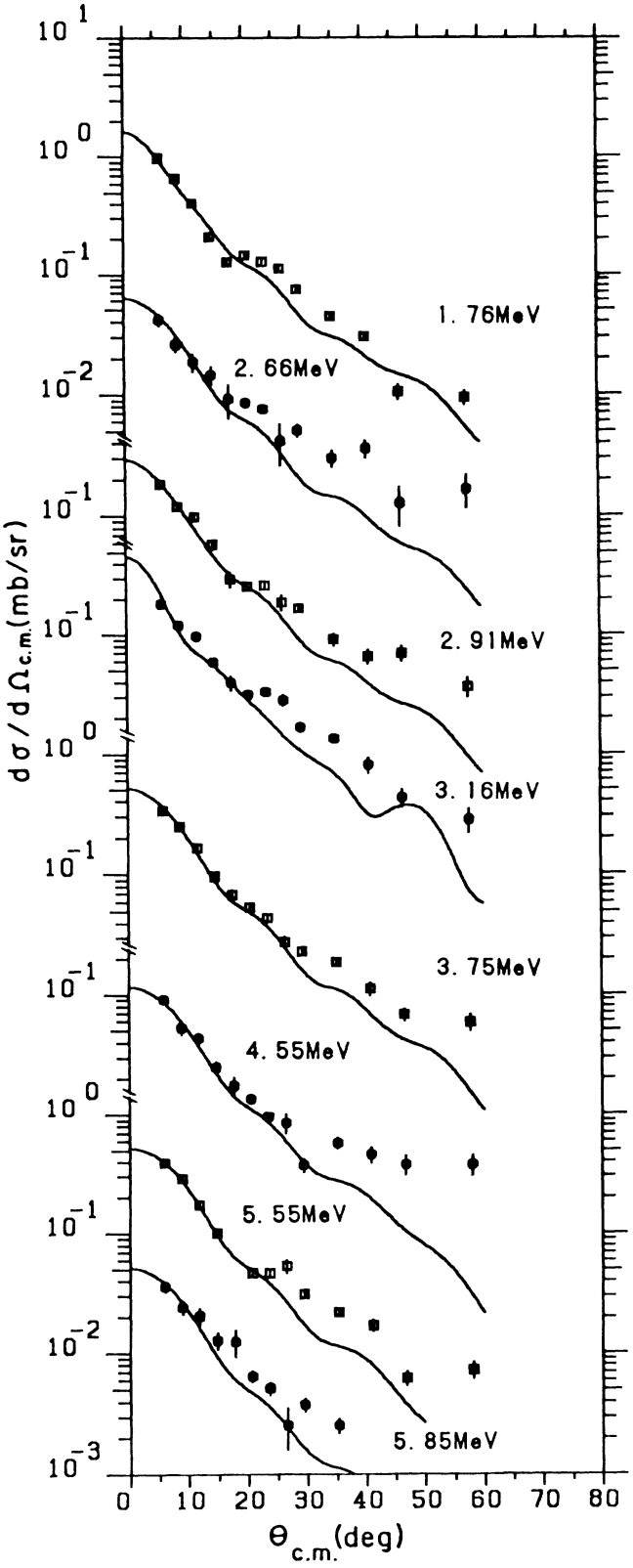

FIG. 14. Angular distributions of the (α,t) cross sections for the 2^+ states in ^{26}Al. Solid curves are EFR-DWBA calculations carried out with the spectroscopic factors in Table V. Cross sections for the 3.751 MeV 2_4^+ and the 3.754 MeV 0_2^+, $T=1$ states are combined ones for the doublet and compared to the summed curve for these states.

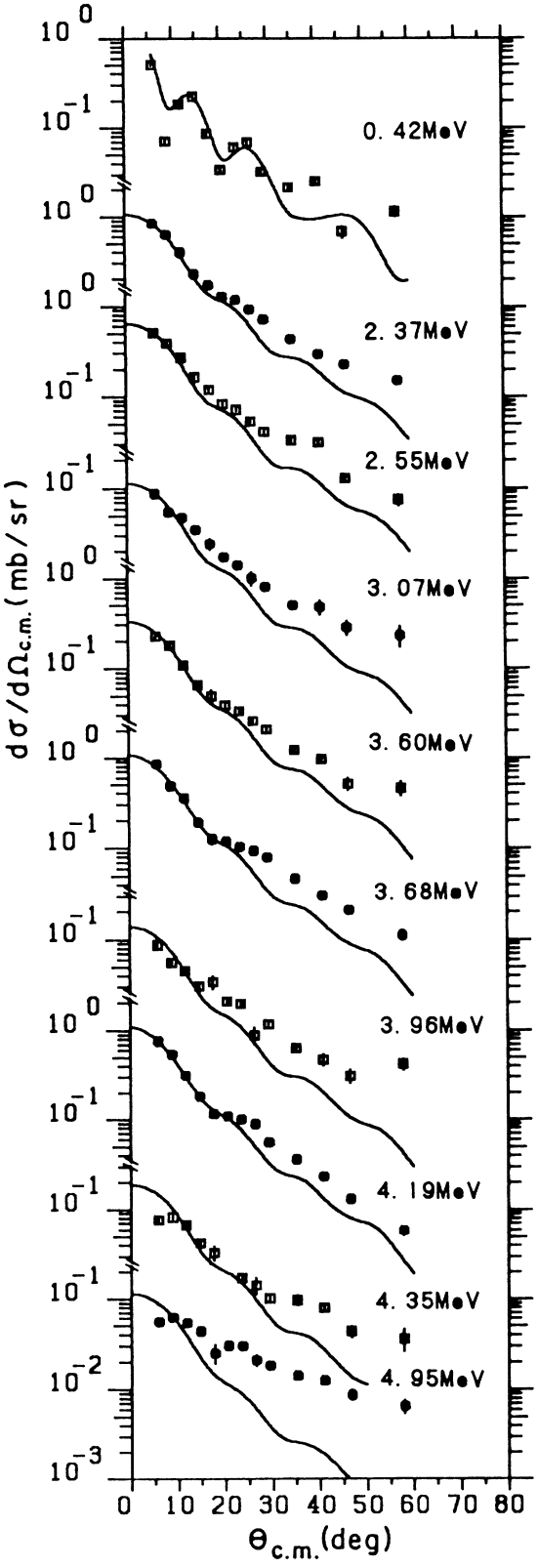

FIG. 15. Angular distribution of the (α,t) cross sections for the 3^+ states in ^{26}Al. Solid curves are EFR-DWBA calculations carried out with the spectroscopic factors in Table V.

G. Sum rules for the transition to the positive-parity states

The $(\alpha,{}^3\mathrm{He})$ and (α,t) reactions on ^{25}Mg can sense the number of the neutron and proton holes in the ground state of ^{25}Mg, respectively. The usefulness of these reactions as probes for the spectroscopic study of nuclear structure was demonstrated in the present work. Namely the cross sections for the lowlying states in ^{26}Al or ^{26}Mg,

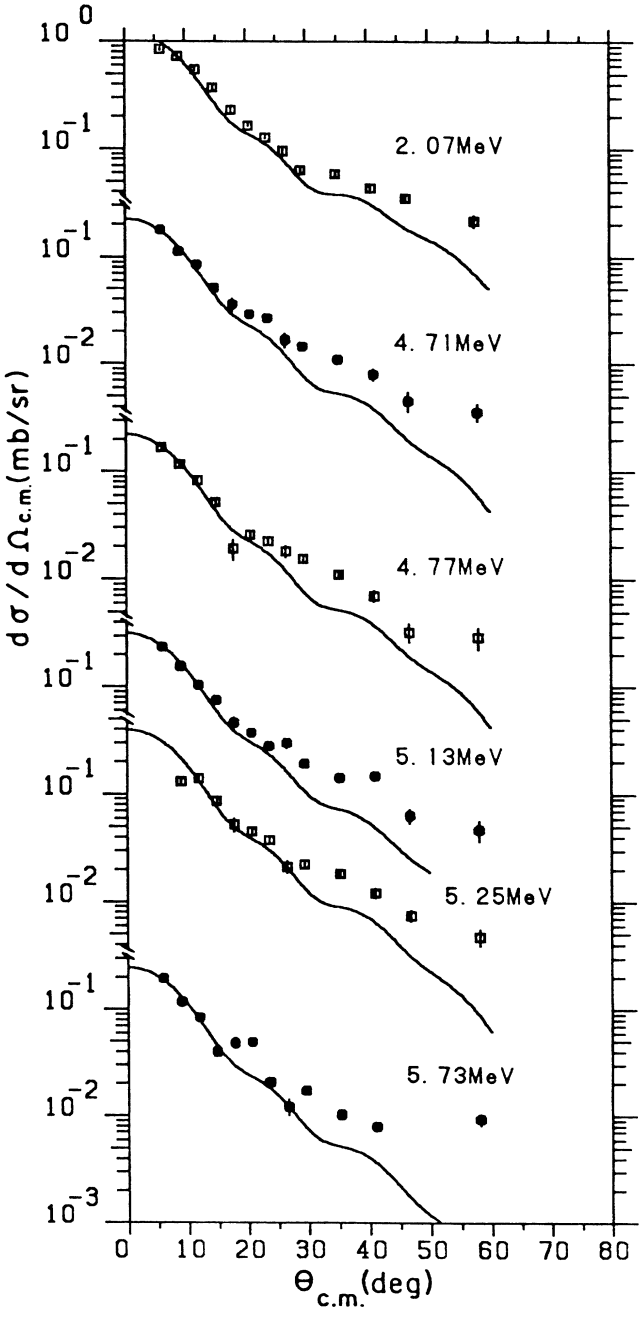

FIG. 16. Angular distributions of the (α,t) cross sections for the 4^+ states in ^{26}Al. Solid curves are EFR-DWBA calculations carried out with the spectroscopic factors in Table V. Cross sections for the 2.07 MeV triplet are combined ones for the 2.068 MeV 4_1^+, the 2.069 MeV 2_1^+, $T=1$ and the 2.072 MeV 1_3^+ states and compared to the summed curve for the three states.

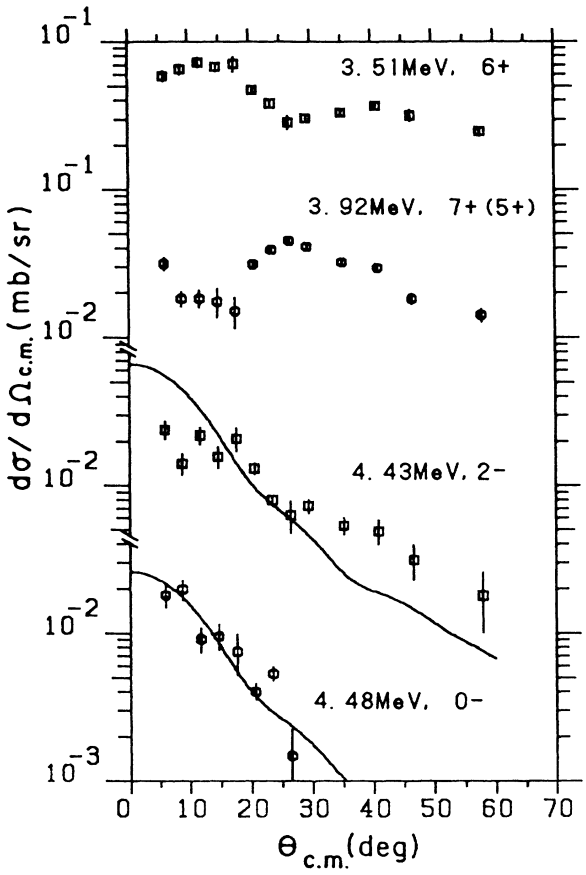

FIG. 17. (α,t) cross sections for the 3.51 and 3.92 MeV states with positive-parity and for the 4.43 MeV, 2^- and the 43.48 MeV, 0^- states. Solid curves for the 2^- and the 0^- states are DWBA calculations for the $0f_{7/2}$ and $0f_{5/2}$ transfers, respectively.

TABLE VI. Spectroscopic information for the negative-parity states in ^{26}Al. The $0f_{7/2}$ transfer is assumed except for the 0^- state, for which the $0f_{5/2}$ orbit is used.

E_x (MeV)	$J^\pi;T$	Spectroscopic factor (α,t)[a] 50 MeV	(α,t)[b] 81 MeV	$(^3\text{He},d)$[c] 55 MeV
6.89	$6^-;0$	0.13	0.16	0.13
9.26	$6^-;1$	0.17	0.20	0.17
6.08	$5^-;0$	0.29	0.32	0.31
8.01	$5^-;1+(0)$	0.11	0.14	0.10
8.06	$5^-;1+(0)$	0.15	0.19	0.18
5.39	$4^-;0$	0.15	0.10	0.10
5.68	$4^-;0$	0.20		
7.35	$4^-;1+0$	0.12		
7.41	$4^-;0+1$	0.09		
4.43	2^-	0.03		
4.48	0^-	0.06		

[a]The results for the states about $E_x=5$ MeV are obtained by using the previous data reported in Ref. 12.
[b]Reference 7.
[c]Reference 22.

whose structures are believed to be simple, were excellently reproduced in absolute values by the present DWBA analyses with the spectroscopic factors predicted from the shell model. Besides, the spectroscopic factors for the proton stripping to the 6^- and 5^- states in ^{26}Al are consistent within a deviation of 20% independently of the used reactions as seen in Table VI. Thus we estimate the ambiguity of the present DWBA analyses of the $(\alpha,^3\text{He})$ and (α,t) reactions on ^{2}Mg to be 20% in the absolute values and about 10% in the relative values. Here we will deduce the number of the holes from the results in Tables I–III and V and in Ref. 12.

The numbers of the neutron and proton holes are related to the spectroscopic factors as follows:[27]

$$\langle n \text{ holes}\rangle = \sum \frac{2J_f+1}{2J_i+1} S_+ , \tag{5}$$

$$\langle p \text{ holes}\rangle = \frac{2T_i}{2T_i+1} \sum \frac{2J_f+1}{2J_i+1} S_- + \frac{1}{2T_i+1} \sum \frac{2J_f+1}{2J_i+1} S_+ , \tag{6}$$

where S_+ and S_- mean the spectroscopic factors for the T_{upper} and T_{lower} states in final nuclei. Experimental angular distribution shapes for the ^{25}Mg $(\alpha,^3\text{He})$ and (α,t) reactions are insensitive to the difference of $0d_{5/2}$ and $0d_{3/2}$ transfers and we cannot distinguish the spectroscopic factor S^i_{expt} for $j=\frac{5}{2}$ and $\frac{3}{2}$ transfers. However, we speculated them by comparing the experimental cross sections to the shell model predictions:

$$S^J_{\text{expt}} = S^J_{\text{calc}} \sigma_{\text{expt}}/\sigma_{\text{calc}} , \tag{7}$$

where S^J_{calc} and $\sigma_{\text{expt}}/\sigma_{\text{calc}}$ are defined in Sec. III.

Obtained results are compared to the shell model[3] and to the pure j-j coupling model in Table VII, where the values in the columns of shell model and experiment are deduced from the spectroscopic factors for the positive-parity states of known spin. Those in the parentheses are for all the positive-parity states in ^{26}Mg and ^{26}Al observed through the present and the previous[12] work. The experimental value for the $0d_{5/2}$ neutron hole has a good agreement with the shell model calculation, and the $0d_{5/2}$ proton hole has a 10% larger value than the calculation. The 10% larger value than the calculation are also seen for the $1s_{1/2}$ holes, while those for the $0d_{3/2}$ holes have 30% or more larger strength than the calculation.

Comparison with the pure j-j coupling scheme tells us important facts: The numbers of the $0d_{5/2}$ neutron and proton holes are larger by factors of 1.5 and 1.1, respectively, than the simple model's prediction. Namely the $0d_{5/2}$ neutron shell orbit has a larger configuration mixture with the $1s_{1/2}$ and $0d_{3/2}$ neutron shells than the $0d_{5/2}$ proton shell orbit does with the $1s_{1/2}$ and $0d_{3/2}$ proton shells. The observed neutron holes have been summed up to the limit of 7, suggesting that the *sd* shell neutron holes are confined in the region of excitation energy below 11 MeV in ^{26}Mg. Hence the positive-parity states in ^{26}Mg above $E_x=11$ MeV seems to have

TABLE VII. Sum rules for the $(\alpha,{}^3\mathrm{He})$ and (α,t) reactions on ^{25}Mg leading to the positive parity states. The sum-rule values in parentheses are obtained by adding the results in Table III and in Ref 12. Namely they cover the data at $E_x=0$–11 MeV in ^{26}Mg and at $E_x=0$–9 MeV in ^{26}Al, while the sum-rule values without parentheses are for $E_x=0$–6 MeV.

	Neutron holes			Proton holes		
Shell orbits	Pure j-j coupling	Shell model[a]	Experiment[b]	Pure j-j coupling	Shell model[a]	Experiment[b]
$0d_{5/2}$	1	1.49	1.49	2	2.15	2.29
$1s_{1/2}$	2	1.08	1.23	2	1.04	1.19
			(2.2)			
$0d_{3/2}$	4	2.03	2.99	4	1.47	1.92
			(4.0)			(2.38)
⟨Sum⟩	⟨7⟩	⟨4.60⟩	⟨5.71⟩	⟨8⟩	⟨4.66⟩	⟨5.4⟩
			⟨(7.7)⟩			⟨(5.9)⟩

[a]Deduced from the calculated spectroscopic factors in Tables I and V and from those for the 1^+ states in ^{26}Mg.
[b]Deduced from the equation $S^J_{\mathrm{expt}}=S^J_{\mathrm{calc}}\sigma_{\mathrm{expt}}/\sigma_{\mathrm{calc}}$ by using the values for S^J_{calc} and $\sigma_{\mathrm{expt}}/\sigma_{\mathrm{calc}}$ in Tables I and V, and from the values in Table II.

configuration mixings with other than the *sd* shell orbits. Such an example was demonstrated for the 7^+ states of ^{26}Al in our previous work[28] on the ^{24}Mg (α,d) ^{26}Al reaction.

The shell model calculation predicts the same spectroscopic factor for each of the analog states in ^{26}Mg and ^{26}Al. This equality holds for the 2^+_1, and 4^+_1, $T=1$ states as seen in Tables I and V. However, the ratios of the experimental to the calculated cross sections for the 0^+_1 and 3^+_1, $T=1$ states in ^{26}Al are 1.3 times larger than those in ^{26}Mg. The larger ratio for ^{26}Al may suggest an effect of deformation as proposed by Takahashi *et al.*[29] Such an effect was also pointed out by Peterson *et al.*[12,22] in terms of the fragmentation of the 6^- states in ^{26}Al and by Glatz *et al.*[30] in terms of the $E2$ transition rates in ^{26}Mg.

V. SUMMARY

The clean spectra for the $(\alpha,{}^3\mathrm{He})$ and (α,t) reactions on ^{25}Mg enabled us to deduce cross sections for 47 states

TABLE VIII. Comparison of spectroscopic information for the analog states in ^{26}Mg and ^{26}Al by referring to the result in Tables I, IV, V, and VI.

	$\sigma_{\mathrm{expt}}/\sigma_{\mathrm{calc}}$ (or S_{expt})[a]		E_x (MeV)[b]	ΔE_x[c]
J^π	^{26}Mg	^{26}Al	in ^{26}Mg	(MeV)
0^+_1	0.76	1.01	0	0.228
2^+_1	1.07	1.07[d]	1.809	0.260
2^+_2	1.0	1.0	2.938	0.222
2^+_3	1.15[e]	1.36	4.332	0.216
2^+_4	2.0	0.89[f]	4.834	0.308
2^+_5	1.07	1.38	5.291	0.254
3^+_1	1.16	1.56	3.941	0.251
4^+_1	1.15[e]	2.25	4.332	0.373
4^+_2	0.80	0.89[f]	4.900	0.232
6^-_1	(0.18)	(0.17)	9.165	0.09
5^-_1	(0.36)	(0.26)[g]	7.952	0.009[g]
4^-_1	(0.40)	(0.21)[h]	7.279	0.10[h]

[a]$\sigma_{\mathrm{expt}}/\sigma_{\mathrm{calc}}$ values for positive-parity states and S_{expt} values for negative-parity states.
[b]E_x values for positive-parity states are cited from Ref. 9 and those for other states are cited from the present result.
[c]$\Delta E_x=E_x(^{26}\mathrm{Al})-E_x(^{26}\mathrm{Mg})$.
[d]Combined value for the 4^+_1, 2^+_1; $T=1$ and 1^+_3 states in ^{26}Al.
[e]Combined value for the $T=1$ 2^+_3 and 4^+_1 states in ^{26}Mg.
[f]Combined value for the $T=1$, 2^+_4 and 4^+_2 states in ^{26}Al.
[g]Combined for the 8.01 MeV and 8.06 MeV 5^- states in ^{26}Al.
[h]Combined for the 7.35 MeV and 7.41 MeV 4^- states in ^{26}Al.

of ^{26}Mg and 45 states of ^{26}Al in the region of excitation energy up to 11 MeV and 9 MeV, respectively. Although some of the cross sections were as small as $\frac{1}{100}$ of those for the ground states of ^{26}Mg and ^{26}Al, their angular distribution shapes were well reproduced by the DWBA calculations. The fact helped us to carry out detailed comparison of the cross sections to those predicted from Wildenthal's shell model calculation. Thus we found that the model can describe excellently the spectroscopic factors for the one-nucleon transfer to most of the positive-parity states in ^{26}Mg and ^{26}Al. Exceptions were found for the transitions to the 2_6^+, 3_6^+, 3_7^+, and 4_4^+ states in ^{26}Al. The strengths for the transitions to these states have deviations of factors of 3 or more from the shell model predictions. Sum rules in Table VII suggest to us that the deviation comes from the poor description of the $0d_{3/2}$ amplitudes in these high-lying positive-parity states.

Furthermore, large deviations between the shell model prediction and the experiment were seen for the 1^+ states in ^{26}Mg, whereas the experimental cross sections for the 1^+ states in ^{26}Al were in excellent agreement with the theory.

We could obtain $(\alpha,{}^3\mathrm{He})$ cross sections for the 1^+ states that are proposed around $E_x=10$ MeV through the (p,p') scattering.[8] The shell model calculation also predicts such a population of 1^+ states in ^{26}Mg. However, the summed spectroscopic factors for the 1^+ states were found to be 2.5 times larger than the prediction. The $(\alpha,{}^3\mathrm{He})$ cross sections for these 1^+ states have angular distribution shapes much different from the $\Delta L=2$ transfer. There remains a possibility that multistep processes through the inelastic scattering might have produced the discrepancy. More serious discrepancy is seen for the 5.69 MeV 1_1^+ state in ^{26}Mg, which has a spectroscopic factor 46 times larger than the predicted value.

The shell model describes the 1_1^+ state of ^{26}Mg to have a structure of

$$(0.04D5+0.05D3)|^{25}\mathrm{Mg}(\tfrac{5}{2}_1^+)\rangle$$

$$+(0,15S1-0.17D3)|^{25}\mathrm{Mg}(\tfrac{1}{2}_1^+)\rangle\ ,$$

where $D5$, $D3$, and $S1$ symbolize the $0d_{5/2}$, $0d_{3/2}$, and $1s_{1/2}$ single-particle components, respectively. The large component coupled to the $\frac{1}{2}^+$ state in ^{25}Mg cannot be sensed by the ^{25}Mg $(\alpha,{}^3\mathrm{He})$ ^{26}Mg reaction. Hence the model predicts small $(\alpha,{}^3\mathrm{He})$ cross section for the 1_1^+ state. However, the experimental cross sections, whose angular shape is well fitted by the $\Delta L=2$ transfer, suggest that the 1_1^+ state should have larger amplitudes coupled to the $\frac{5}{2}^+$ ground state in ^{25}Mg than the shell model describes.

Spectroscopic factors for the analog states in ^{26}Mg and ^{26}Al were also compared to each other not only for the positive-parity states but also for the negative-parity states. They are summarized in Table VIII together with the difference of excitation energies between the analog states. The same strength was observed for the 6_1^-, $T=1$ states. The equality was seen for the 2_1^+, $T=1$ states and for the 4_1^+, $T=1$ states, too. However the strengths for the 5_1^- and 4_1^- states in ^{26}Mg were fragmented into the two levels in ^{26}Al with each spin value. The spectroscopic factors for the 0_1^+ and 3_1^+, $T=1$ states in ^{26}Al were found to be 1.3 times larger than those for the analog states in ^{26}Mg. The information in the table suggests a presence of higher-order configuration mixings in the analog states of these nuclei.

In conclusion, the $(\alpha,{}^3\mathrm{He})$ and (α,t) reactions on ^{25}Mg were found to be an excellent probe for the spectroscopic study of the nuclear structure of ^{26}Mg and ^{26}Al. Wildenthal's shell model calculations were found to be powerful to describe the spectroscopic nature of the positive-parity states in these nuclei as well as the excitation energies. We have shown, however, that the model has some points to be improved in terms of the 1^+ states in ^{26}Mg and the distribution of the $0d_{3/2}$ components.

ACKNOWLEDGMENTS

We are obliged to Prof. R. J. Peterson of the University of Colorado, for encouraging us throughout this work and for critical reading of the manuscript. We are also grateful to Prof. T. Suzuki for encouraging discussions with us and to Dr. I. Sugai for preparation of a thin ^{25}Mg target. Numerical calculations were carried out with the central computers at the Research Center for Nuclear Physics, Osaka University, at the Institute for Nuclear Study, the University of Tokyo, and at the Kantogakuin University.

[1]P. M. Endt, P. de Wit, C. Alderliesten, and B. H. Wildenthal, Nucl. Phys. **A487**, 221 (1988).

[2]P. M. Endt, P. de Wit, and C. Alderliesten, Nucl. Phys. **A476**, 333 (1988); **A459**, 61 (1986).

[3]B. H. Wildenthal, Prog. Part. Nucl. Phys. **11**, 5 (1984); in *Proceedings of the Yamada Conference on Nuclear Weak Process and Nuclear Structure, Osaka,* 1989, edited by M. Morita *et al.* (World Scientific, Singapore, 1989), p. 314.

[4]R. R. Betts, H. T. Fortune, and D. J. Pullen, Nucl. Phys. **A299**, 412 (1978).

[5]H. F. R. Arciszewski, E. A. Bakkum, C. P. M. van Engelen, P. M. Endt, and P. Kamermans, Nucl. Phys. **A430**, 234 (1984).

[6]J. J. Kraushaar, M. Fujiwara, K. Hosono, M. Kondo, H. Sakai, M. Tosaki, M. Yasue, S. I. Hayakawa, and R. J. Peterson, Phys. Rev. C **34**, 1530 (1986).

[7]R. J. Peterson, B. L. Clausen, J. J. Kraushaar, H. Nann, W. W. Jacob, R. A. Lindgren, and M. S. Plum, Phys. Rev. C **33**, 31 (1986).

[8]G. M. Crawley, C. Djalali, N. Marty, M. Morlet, A. Willis, N. Anantaraman, B. A. Brown, and A. Galonsky, Phys. Rev. C **39**, 311 (1986).

[9]P. M. Endt and C. van der Leun, Nucl. Phys. **A310**, 208 (1978).

[10]S. Kato, M. H. Tanaka, and T. Hasegawa, Nucl. Instrum. Methods **154**, 19 (1978).

[11]M. H. Tanaka, S. Kubono, and S. Kato, Nucl. Instrum. Methods **195**, 509 (1982).

[12]M. Yasue, H. Sato, T. Hasegawa, J. Takamatsu, A. Terakawa, T. Nakagawa, and R. J. Peterson, Phys. Rev. C **39**, 2159 (1989).
[13]M. Yasue and T. Wada, Institute for Nuclear Study, University of Tokyo, Report No. 670, 1988 (unpublished).
[14]M. Yasue, T. Tanabe, S. Kubono, J. Kokame, and M. Igarashi, Nucl. Phys. **A391**, 377 (1982).
[15]TWOFNR, An exact-finite-range DWBA code written by M. Igarashi (unpublished).
[16]M. Igarashi, Phys. Lett. **78B**, 379 (1978).
[17]INS, a code for shell model calculations written by K. Ogawa (unpublished).
[18]DWUCK4, a zero-range DWBA code written by P. D. Kunz, University of Colorado (unpublished).
[19]F. H. Lutz and S. F. Eccles, Nucl. Phys. **A88**, 513 (1966).
[20]H. Fuchs, K. Grabish, P. Kraaz, and G. Röschert, Nucl. Phys. **A110**, 65 (1968).
[21]A. Weidinger, R. H. Siemssen, G. C. Morrison, and B. Zeidman, Nucl. Phys. **A110**, 65 (1968).
[22]R. J. Peterson, M. Yasue, M. H. Tanaka, T. Hasegawa, K. Nishimura, H. Ohnuma, H. Shimizu, K. Ieki, H. Toyokawa, and S. I. Hayakawa, Phys. Rev. C **38**, 1130 (1988).
[23]L. W. Fagg, Rev. Mod. Phys. **47**, 683 (1975).
[24]M. Yasue *et al.*, Nucl. Phys. **A510**, 285 (1990).
[25]M. A. Plum, Ph. D. thesis, University of Massachusetts, 1985 (unpublished).
[26]R. E. Segel, A. Amusa, D. F. Geesamen, R. D. Lawson, B. Zeidman, C. Olmer, A. D. Bacher, G. T. Emery, C. W. Golver, H. Nann, W. P. Jones, S. Y. van der Werf, and R. A. Lindgren, Phys. Rev. C **39**, 749 (1989).
[27]J. B. French and M. H. Macfarlane, Nucl. Phys. **26**, 168 (1961).
[28]M. Yasue, H. Sato, M. H. Tanaka, T. Hasegawa, T. Tanabe, K. Nishimura, H. Ohnuma, H. Schimizu, K. Ieki, H. Toyokawa, K. Ogawa, S. I. Hayakawa, and R. J. Peterson, Phys. Rev. C **40**, 1933 (1989).
[29]N. Takahashi *et al.*, Phys. Rev. C **23**, 1305 (1981).
[30]F. Glatz *et al.*, Z. Phys. A **324**, 187 (1986).